



Subcriticality estimation by extended Kalman filter technique in transient experiment with external neutron source at Kyoto University Critical Assembly

Masao Yamanaka^{1,a} , Kenichi Watanabe², Cheol Ho Pyeon¹

¹ Research Center for Safe Nuclear System, Institute for Integrated Radiation and Nuclear Science, Kyoto University, Asashiro-nishi, Kumatori-cho, Sennan-gun, Osaka 590-0494, Japan

² Department of Applied Energy Engineering, Graduate School of Engineering, Nagoya University, Furo-cho, Chikusa-ku, Nagoya 464-8603, Japan

Received: 8 May 2019 / Accepted: 8 February 2020 / Published online: 18 February 2020

© Società Italiana di Fisica and Springer-Verlag GmbH Germany, part of Springer Nature 2020

Abstract The monitoring subcriticality by the extended Kalman filter (EKF) is evaluated in the presence of an external neutron source through transient analyses and compares with that by inverse kinetic method at Kyoto University Critical Assembly. Throughout the transient experiment, subcriticality is deduced with the use of neutron counts measured every 1 s. For ensuring the initial condition of the EKF technique, the basic transient experiment is carried out by dropping a control rod into the core at a critical state, and the result by the EKF technique shows remarkably accurate subcriticality as compared with the reference value obtained by the rod drop method with less fluctuation than by the inverse kinetic method. In the ADS transient experiment with the 14 MeV stable neutron source, the subcriticality is set as target subcriticality of the accelerator-driven system ($k_{\text{eff}} = 0.97$); the external neutrons are then injected from outside the core. The EKF technique reveals significantly good agreement with MCNP6.1, whereas subcriticality by the inverse kinetic method fluctuates widely during the transient experiment. Thus transient experiment shows that the EKF technique is applicable to subcriticality monitoring with a high time resolution and a high degree of precision.

1 Introduction

Critical safety in operating nuclear systems (including nuclear power plants and spent fuel storage pools) is a prerequisite to its experimental evaluation by neutron multiplication (M) and its numerical evaluation of the criticality by neutronic calculations. Criticality accidents at the constitution of a critical core can be prevented by starting fuel loading at subcritical state long before the critical state, and by plotting $1/M$ curve at each loading step. The reactivity monitoring system has been considered for reactivity variation by burnup and accidental rapid induction based on the one-point kinetic equation. In the accelerator-driven system (ADS), a new nuclear system, reactor monitoring methodology is required to take into account the effect of external neutron sources, since ADS is operated at a subcritical state with a neutron source. Here, the neutron multiplication factor k_{eff} was revealed to have a correlation with

^a e-mail: m-yamanaka@rri.kyoto-u.ac.jp

the neutron spectrum of the subcritical core [1]. For intense reactivity variation, evaluations by the one-point kinetic equation are considered useful with kinetic parameters representing the neutron spectrum [2–4].

On-line monitoring of reactivity has been deduced in real time by the inverse kinetic method on the basis of the one-point kinetic equation with measured neutron signals in the core [5,6]. The inverse kinetic method had been theoretically extended to apply to thermal reactor cores by considering thermal feedback to the one-point kinetic equation [7]. Also, small reactivity has been successfully measured by the inverse kinetic method in real time, demonstrating the flexible applicability to reactor monitoring [8]. Here, measurements by one-point kinetic equation have been validated through the subcriticality evaluation with the pulsed-neutron source histogram [9] and the methodology by the inhour equation [10]. Accuracy, however, is decreased by low neutron counts equal to those at background level, resulting in the fluctuation of monitoring values. Thus, the applicability of the Kalman filter technique based on the Bayesian estimation was indicated with the consideration with one group of delayed neutrons to the one-point kinetic equation, although the fluctuation was observed in the reactivity monitoring by background noise at low neutron counts [11]. The filtering technique is conducive to extract a likelihood solution by predicting the uncertainty of measured neutron counts beforehand without complex calculations.

While the Kalman filter technique is inapplicable to the nonlinearity of the state space model, the extended Kalman filter (EKF) technique that includes first-order approximation of the Taylor expansion was comparable to the inverse kinetic method in monitoring reactivity [12]. Here discussed was a comparative study in terms of numerical experiments of transient (control rod insertion into a critical core) and time-dependent neutron calculations. The system noise for EKF was then artificially generated by numerical neutron flux distributions. The performance of EKF was demonstrated by reducing the fluctuation of reactivity to low neutron counts and compared with the inverse kinetic method; determination of measurement uncertainty was, however, difficult. Furthermore, the particle filter technique is applicable to nonlinearity by the most likelihood method with measured results and system noise estimated by numerical analyses, demonstrating good results of simultaneous estimation of not only the reactivity but also effective delayed neutron fraction (β_{eff}) and generation time (Λ) in real time [13].

Subcriticality monitoring at ADS operation is evaluated every 3 s [14] and requires sufficient neutron counts for accurate measurement by the inverse kinetic method and the pulsed-neutron source method. The particle filter is effective for low neutron counts in a strong nonlinear system; however, its application is considered difficult due to the large uncertainty induced by nuclear data and information of geometry and materials in general since predicted accuracy is strongly affected by the accuracy of nuclear calculations. For subcriticality monitoring, the EKF technique has a possibility to be applicable to the extended methodology for the measurements in the presence of external neutron sources. The objective of this study was to evaluate the applicability of the EKF technique for monitoring subcriticality during the ADS operation in the presence of external neutron sources. The theoretical background of EKF is described in Sect. 2; the experimental settings of transient experiments at critical and subcritical states are shown in Sect. 3; the applicability of the EKF technique to the critical experiment and the ADS transient experiment is examined in Sect. 4; the conclusion is summarized in Sect. 5

2 Theoretical background

In EKF, the state space $\mathbf{x}(k)$ in time step k (1, 2, ...) and the observation equation $\mathbf{y}(k)$ are expressed, as follows:

$$\mathbf{x}(k + 1) = \mathbf{f}(\mathbf{x}(k)) + \mathbf{b}v(k), \tag{1}$$

$$y(k) = h(\mathbf{x}(k)) + w(k), \tag{2}$$

where \mathbf{f} is the matrix expressing state space, \mathbf{b} the vector distributing system noise, v the (white) system noise (average = 0.0, variance = σ_v^2), h the observable matrix, w the observation noise (average = 0.0, variance = σ_w^2). EKF is applicable to nonlinearity with first-order approximation by considering derivative \mathbf{A} and \mathbf{c}^T , as follows:

$$\mathbf{A}(k) = \left. \frac{\partial \mathbf{f}(\mathbf{x}(k))}{\partial \mathbf{x}} \right|_{\mathbf{x}=\hat{\mathbf{x}}^-(k)} \tag{3}$$

$$\mathbf{c}^T(k) = \left. \frac{\partial h(\mathbf{x}(k))}{\partial \mathbf{x}} \right|_{\mathbf{x}=\hat{\mathbf{x}}^-(k)}, \tag{4}$$

where $\hat{\mathbf{x}}^-$ is the priori estimate (prediction estimation of \mathbf{x} in time step k based on collected experience until time $k - 1$). The procedure of the general Kalman filter technique is divided into a prediction step and a filtering step. For the prediction step, the priori estimate is evaluated with the use of state estimate $\hat{\mathbf{x}}$ in a previous time step, as follows:

$$\hat{\mathbf{x}}^-(k) = \mathbf{f}(\hat{\mathbf{x}}(k - 1)). \tag{5}$$

Next, the priori error covariance matrix \mathbf{P}^- is evaluated, as follows:

$$\mathbf{P}^-(k) = \mathbf{A}(k)\mathbf{P}(k - 1)\mathbf{A}^T(k) + \sigma_v^2\mathbf{b}\mathbf{b}^T, \tag{6}$$

where \mathbf{P} is a posteriori error covariance matrix. Here, in the first step, initial values of $\hat{\mathbf{x}}^-$ and \mathbf{P}^- are requisite to perform EKF. For the filtering step, Kalman gain \mathbf{g} is determined, as follows:

$$\mathbf{g}^-(k) = \frac{\mathbf{P}^-(k)\mathbf{C}(k)}{\mathbf{C}^T(k)\mathbf{P}^-(k)\mathbf{C}(k) + \sigma_w^2}. \tag{7}$$

The state estimate is evaluated with the use of observation results and the priori state estimate by the most likelihood parameter \mathbf{g} , as follows:

$$\hat{\mathbf{x}}(k) = \hat{\mathbf{x}}^-(k) + \mathbf{g}(k)\{y(k) - h(\hat{\mathbf{x}}^-(k))\}. \tag{8}$$

Finally, in the next step, the posteriori error covariance matrix is prepared, as follows:

$$\mathbf{P}(k) = \{\mathbf{I} - \mathbf{g}(k) - \mathbf{C}^T(k)\}\mathbf{P}^-(k). \tag{9}$$

In this study, initial values of Eqs. (5) and (6) were prepared by the inverse kinetic method based on one-point kinetic equations, as follows:

$$\frac{dn(t)}{dt} = \frac{\rho(t) - \beta_{\text{eff},i}}{\Lambda}n(t) + \sum_{i=1}^6 \lambda_i C_i(t), \tag{10}$$

$$\frac{dC_i(t)}{dt} = \frac{\beta_{\text{eff}}}{\Lambda}n(t) + \lambda_i C_i(t), \tag{11}$$

where n is the neutron density, ρ the reactivity, $\beta_{\text{eff},i}$ the effective delayed neutron fraction of the i -th group, λ_i the delayed neutron decay constant of the i -th group, C_i the density of

delayed neutron precursor. For obtaining reactivity in Eq. (10) at every time step, the time variation of C_i in Eq. (11) is expressed with backward difference, as follows:

$$\frac{C_i(k) - C_i(k - 1)}{\Delta k} = \frac{\beta_{\text{eff},i}}{\Lambda} n(k) + \lambda_i C_i(k) \quad (k = 2, 3, \dots), \tag{12}$$

ρ is obtained by substituting $C_i(k)$ in Eq. (12) for Eq. (10), as follows:

$$\begin{aligned} \rho(t) = & \left. \frac{dn(t)}{dt} \right|_{t=1} \frac{\Lambda}{n(k)} + \beta_{\text{eff}} \\ & - \frac{\Lambda}{n(k)} \sum_{i=1}^6 \frac{\lambda_i}{1 + \lambda_i \Delta k} \left\{ \frac{\beta_{\text{eff},i}}{\Lambda} n(k) \Delta k C_i(k - 1) \right\}. \end{aligned} \tag{13}$$

Here, when an experiment is assumed to have started at a critical state, the initial value (at $k = 1$) of C_i is estimated, as follows:

$$C_i(1) = \frac{\beta_{\text{eff},i}}{\lambda_i \Lambda} n(1). \tag{14}$$

When monitoring subcriticality by the EKF technique in the critical core, the result of Eq. (14) was used as the initial values.

In ADS experiments with a stable external neutron source, the one-point kinetic equation on neutron derivative is changed, as follows:

$$\frac{dn(t)}{dt} = \frac{\rho(t) - \beta_{\text{eff}}}{\Lambda} n(t) + \sum_{i=1}^6 \lambda_i C_i(t) + S_{\text{eff}}, \tag{15}$$

where S_{eff} is effective strength of the stable neutron source. By substituting C_i in Eq. (12) for Eq. (15), as same procedure in Eq. (13), ρ is expressed in ADS experiments, as follows:

$$\begin{aligned} \rho(t) = & \left. \frac{dn(t)}{dt} \right|_{t=1} \frac{\Lambda}{n(k)} + \beta_{\text{eff}} \\ & - \frac{\Lambda}{n(k)} \sum_{i=1}^6 \frac{\lambda_i}{1 + \lambda_i \Delta k} \left\{ \frac{\beta_{\text{eff},i}}{\Lambda} n(k) \Delta k C_i(k - 1) \right\} \\ & - \frac{\Lambda}{n(k)} S_{\text{eff}}. \end{aligned} \tag{16}$$

Here, assuming that the external neutron source is stable, S_{eff} was determined as follows:

$$S_{\text{eff}} = -\frac{\rho(1)}{\Lambda} n(1). \tag{17}$$

When monitoring subcriticality by the EKF technique with the external neutron source, $\rho(1)$, C_i in Eq. (14) and S_{eff} in Eq. (17) were used as the initial values.

3 Experimental settings

3.1 Critical core

Transient experiments were carried out in the uranium-polyethylene (EE1) core at Kyoto University Critical Assembly (KUCA), as shown in Fig. 1. The core was constituted by fuel

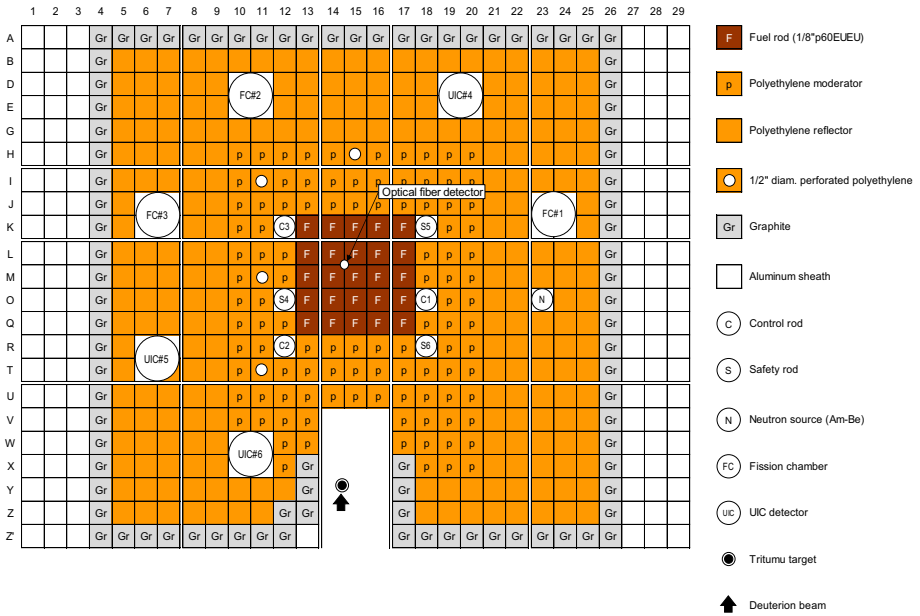


Fig. 1 Description of critical core with 14 MeV neutrons at KUCA

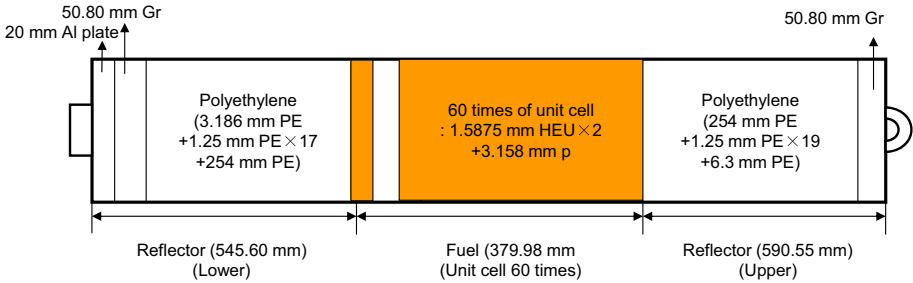


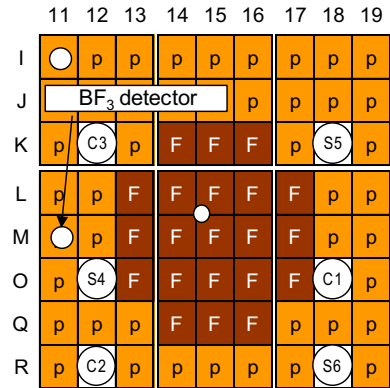
Fig. 2 Schematic of fuel rods “F” in Fig. 1 (1/8”p 60EUEU)

rods (1/8”p60EUEU), made of a highly enriched uranium (HEU; 50.8 × 50.8 × 1.5875 mm) and a polyethylene moderator (p; 50.8 × 50.8 × 3.158 mm) in an aluminum sheath 54 × 54 × 1524 mm, as shown in Fig. 2. The core spectrum was hard in the polyethylene-moderated core at KUCA [an H/U (hydrogen/uranium) ratio of approximately 50 in the thermal reactor].

Time evolution of neutron signals was obtained by an optical fiber detector (Eu:LiCaAlF6 scintillator) set at the core center for monitoring reactivity based on one-point kinetic approximation (to prevent measuring higher-mode components in neutron flux and variation of detector efficiency)

The transient experiments were conducted after attaining critical state with the C2 control rod (with all the other control and safety rods withdrawn); C1 control rod (Fig. 1) was then dropped from the fully withdrawal position to the fully inserted position. The neutron counts were obtained every 1 s.

Fig. 3 Description of subcritical core with 14 MeV neutrons at KUCA



3.2 Subcritical core

The ADS transient experiment was carried out with the subcritical core at $k_{eff} = 0.97$ (target range of the subcriticality monitoring in ADS), as shown in Fig. 3. The 14 MeV neutrons were generated by the injection of deuteron beam (intensity 0.15 mA, pulsed width 90 μ s and pulsed frequency 100 Hz) onto a tritium target located at (14–15, Y; Fig. 1).

In the preparation of the transient experiment, all control and safety rods were withdrawn, and, 14 MeV neutrons were then injected into the subcritical core. After 500 s, the C1 control rod was (slowly) inserted by actuator-driven mechanism from the fully withdrawal position to the fully inserted position. The BF₃ detector used in this experiment was placed at (12, M; Fig. 3). Time evolution of the neutron count was obtained every 1 s.

4 Transient analyses

4.1 Calibration in critical core

To perform the EKF technique in a time variable system, setting the variance values of system noise and observation noise is requisite to be set. Furthermore, an initial priori error covariance matrix is needed for the calibration of the filter. The validity of the initial conditions in EKF parameters was evaluated by comparing the results by the rod drop method with those of the EKF technique, and those of the inverse kinetic method in the transient experiment (C1 rod drop) with the critical core.

Numerical analyses of kinetic parameters were conducted with the use of MCNP6.1 [15] together with ENDF/B-VII.1 [16] (total histories was 5E+08 (5E+05 history per cycle and 1E+03 active cycle)). Variance value of system noise was set only for the reactivity of 8E–08; and, the observation noise was set as for the neutron count obtained at the time step for the variance value. Furthermore, the error covariance matrix was set zero except for the reactivity (1E–07) as the EKF parameters.

Here, the variable on the state space model was set as follows:

$$\mathbf{x}(k) = {}^t (n(k) \ C_1(k) \ C_2(k) \ C_3(k) \ C_4(k) \ C_5(k) \ C_6(k) \ \rho(k)), \quad (18)$$

where, t indicates transposition of the matrix. Furthermore, function $f(\mathbf{x}(k))$ in Eq. (1) is described as follows:

$$f(x(k)) = \begin{pmatrix} n(k) + T \left(\frac{\rho(k) - \beta_{\text{eff}}}{\Lambda} n(k) + \sum_{i=1}^6 \lambda_i C_i(k) \right) \\ C_1(k) + T \left(\frac{\beta_{\text{eff},1}}{\Lambda} n(k) - \lambda_1 C_1(k) \right) \\ C_2(k) + T \left(\frac{\beta_{\text{eff},2}}{\Lambda} n(k) - \lambda_2 C_2(k) \right) \\ C_3(k) + T \left(\frac{\beta_{\text{eff},3}}{\Lambda} n(k) - \lambda_3 C_3(k) \right) \\ C_4(k) + T \left(\frac{\beta_{\text{eff},4}}{\Lambda} n(k) - \lambda_4 C_4(k) \right) \\ C_5(k) + T \left(\frac{\beta_{\text{eff},5}}{\Lambda} n(k) - \lambda_5 C_5(k) \right) \\ C_6(k) + T \left(\frac{\beta_{\text{eff},6}}{\Lambda} n(k) - \lambda_6 C_6(k) \right) \\ \rho(k) \end{pmatrix}, \tag{19}$$

where T is the time resolution according to the forward difference: 1.0 in this study. Finally, function $A(k)$ is expressed as follows:

$$A(k) = \begin{pmatrix} 1 + T \left(\frac{\rho(k) - \beta_{\text{eff}}}{\Lambda} \right) & T\lambda_1 & T\lambda_2 & T\lambda_3 & T\lambda_4 & T\lambda_5 & T\lambda_6 & \frac{Th(x(1))}{\Lambda} \\ T \frac{\beta_{\text{eff},1}}{\Lambda} & 1 - T\lambda_1 & 0 & 0 & 0 & 0 & 0 & 0 \\ T \frac{\beta_{\text{eff},2}}{\Lambda} & 0 & 1 - T\lambda_2 & 0 & 0 & 0 & 0 & 0 \\ T \frac{\beta_{\text{eff},3}}{\Lambda} & 0 & 0 & 1 - T\lambda_3 & 0 & 0 & 0 & 0 \\ T \frac{\beta_{\text{eff},4}}{\Lambda} & 0 & 0 & 0 & 1 - T\lambda_4 & 0 & 0 & 0 \\ T \frac{\beta_{\text{eff},5}}{\Lambda} & 0 & 0 & 0 & 0 & 1 - T\lambda_5 & 0 & 0 \\ T \frac{\beta_{\text{eff},6}}{\Lambda} & 0 & 0 & 0 & 0 & 0 & 1 - T\lambda_6 & 0 \\ 0 & 0 & 0 & 0 & 0 & 0 & 0 & 1 \end{pmatrix}. \tag{20}$$

Note that element (1, 8) in Eq. (20) was approximately $\frac{Th(x(1))}{\Lambda}$ ($h(x(1))$ indicates the initial neutron count in the experiment) instead of $\frac{Tn(k)}{\Lambda}$. This value was introduced to take into account the strong nonlinearity in the model. In the estimate with the use of $\frac{Tn(k)}{\Lambda}$, the results were unreliable and divergent.

The transient experiment was started at the critical state; C1 control rod was then dropped into the core, inducing rapid decrease in the neutron counts shown in Fig. 4. Importantly, the EKF technique reproduced measured count distribution (Fig. 4). The results of subcriticality monitoring revealed fluctuation in the result by the inverse kinetic method shown in Fig. 5, demonstrating that slight variation in the neutron count in the region of the low count rate greatly affected to the estimate of subcriticality. Conversely, the result of the EKF technique was notably decreased the fluctuation notably even after the count rate reached almost zero and the estimated value asymptotically approached the reference value, although the overshoot was found when the variation in subcriticality stopped rapidly.

By the transient experiment in the critical core, the validity of the transient analysis was confirmed with the superiority of the filtering technique in reducing the fluctuation of monitoring values.

Fig. 4 Neutron count rate distribution during C1 drop transient

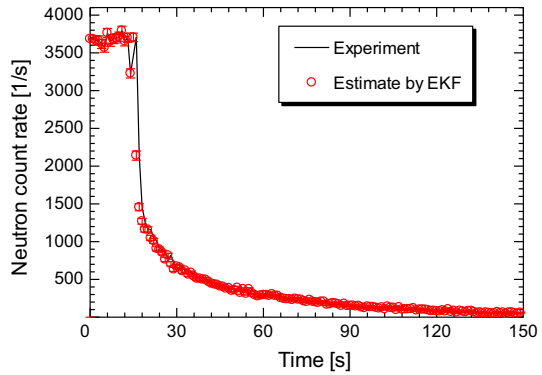
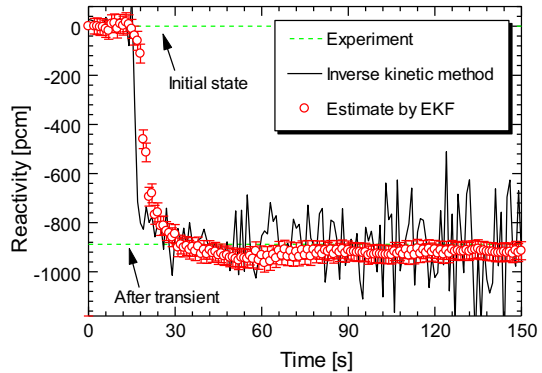


Fig. 5 Comparison of subcriticality monitoring between the inverse method and the EKF technique in C1 rod (worth: - 888 pcm) drop experiment



4.2 Performance evaluation

The objective transient experiment was conducted at the subcritical state in the presence of an external neutron source for evaluating the performance of subcriticality monitoring by the EKF technique, at the same initial condition described in Sect. 4.1. So as to consider the external neutron source in EKF, $T \times S_{eff}$ is appended to element (1) in Eq. (19)

The neutron count distribution was varied gradually compared to the rod drop experiment because of the insertion by actuator drive and kept at a constant value at the end of transient behavior in view of the presence of the external neutron source, as shown in Fig. 6. The estimate by the EKF technique of the neutron counts showed almost the same distribution as of the experiment. In subcriticality monitoring by the inverse kinetic method shown in Fig. 7, the fluctuation in the monitoring values increased remarkably after the transient as the neutron count decreased. In EKF, the monitoring values importantly followed the subcriticality in the transient behavior without fluctuation. Moreover, the estimated subcriticality by the EKF technique was found to be significantly more accurate than that by the inverse kinetic method, demonstrating the validity of estimate by EKF and the reliability of subcriticality monitoring

In the transient experiment with the external neutron source, the S_{eff} values should be considered variable in addition to the detection efficiency since these values can be varied by the insertion of control rods. Thus, to improve monitoring accuracy, in future studies the modeling of the space state equation has to be modified on the basis of S_{eff} and detection efficiency.

Fig. 6 Neutron count rate distribution during C1 drop transient with external neutron source

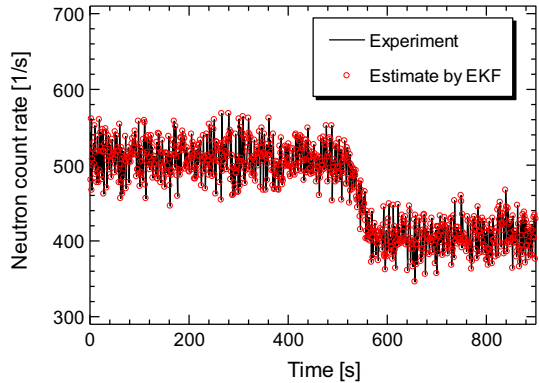
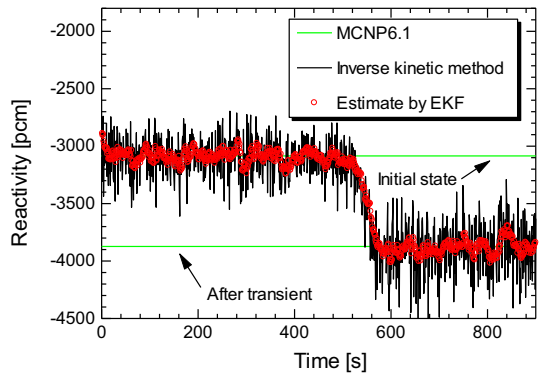


Fig. 7 Comparison of subcriticality monitoring between the inverse method and the EKF technique in ADS transient experiment



5 Conclusion

Transient experiments were carried out to evaluate the performance of subcriticality monitoring by the EKF technique in the presence of an external neutron source. To ensure the conditions in EKF, a basic transient experiment was conducted by dropping the control rod at the critical state. In a comparison of the subcriticality by the inverse kinetic method and the EKF technique, the advantage of EKF was indicated over the robustness of the estimate with good accuracy even at low counts. Additionally, the initial condition used in the filtering technique was confirmed as valid through comparison with measured subcriticality by the rod drop method in the basic transient experiment.

In the transient experiments in the presence of an external neutron source, the EKF technique was applied to subcriticality monitoring (time resolution: 1 s), with the use of the initial condition in the basic experiments. The EKF technique significantly indicated a significant advantage in reducing fluctuation and estimating more accurately compared with the inverse method, demonstrating the applicability to the subcriticality monitor.

Acknowledgements The authors are grateful to Assistant Professor T. Endo of Nagoya University for his invaluable advice in interpretation of system noise used for the extended Kalman filter.

References

1. P. Saracco et al., EPJ Web Conf. **153**, 05017 (2017)
2. M. Carta et al., Nucl. Sci. Eng. **133**, 282 (1999)
3. P. Ravetto et al., Ann. Nucl. Eng. **24**, 303 (1997)
4. F. Peinetti et al., Ann. Nucl. Eng. **33**, 1189 (2006)
5. J.J. Duderstadt, *Nuclear Reactor Analysis*, 1st edn. (Wiley, Hoboken, 1976)
6. S. Dulla et al., Ann. Nucl. Eng. **65**, 433 (2014)
7. R.L. Murray et al., Nucl. Sci. Eng. **18**, 481 (1964)
8. A.M. Gadowski et al., Ann. Nucl. Eng. **6**, 175 (1979)
9. S. Dulla et al., Ann. Nucl. Eng. **101**, 397 (2017)
10. S. Dulla et al., Ann. Nucl. Eng. **87**, 1 (2016)
11. J.C. Venerus et al., Nucl. Sci. Eng. **40**, 199 (1970)
12. Y. Shimazu et al., Ann. Nucl. Eng. **66**, 161 (2014)
13. T. Ikeda et al., Proc. Trans. Am. Nucl. Soc. **118**, 851 (2018)
14. H. Iwamoto et al., J. Nucl. Sci. Technol. **54**, 432 (2017)
15. J. T. Goorley et al., Initial MCNP6 release overview - MCNP6 version 1.0. Los Alamos National Laboratory; LA-UR-13-22934. (2013). <https://doi.org/10.2172/1086758>
16. M.B. Chadwick et al., Nucl. Data Sheets **112**, 2887 (2011)